Article

Not peer-reviewed version

Iron Homeostasis and Reproduction: Unveiling the Microbiome-Gut-Brain-Axis Connection in the Mosquito *Anopheles culicifacies*

Pooja Yadav , Jyoti Rani , Tanvi Singh , Vaishali Saini , Pooja Rohilla , Vartika Srivastava , Gitanjali Tandon , Nirmala Sankhala , Gunjan Sharma , Suchi Tyagi , Sanjay Tevatiya , Seena Kumari * , Rajnikant Dixit *

Posted Date: 3 February 2026

doi: 10.20944/preprints202602.0119.v1

Keywords: mosquito; blood-feeding; iron homeostasis; microbiome; gut-brain axis

Article

Iron Homeostasis and Reproduction: Unveiling the Microbiome-Gut-Brain-Axis Connection in the Mosquito *Anopheles culicifacies*

Pooja Yadav [1,2], Jyoti Rani [1], Tanvi Singh [1,2], Vaishali Saini [1,2], Pooja Rohilla [1,2], Vartika Srivastava [1,2], Gitanjali Tandon [1], Nirmala Sankhala [1,2], Gunjan Sharma [1,2], Suchi Tyagi [1,2], Sanjay Tevatiya [1], Seena Kumari [1]* and Rajnikant Dixit [1,2]*

[1] Laboratory of Host-Parasite Interaction Studies, Department of Vector Genomics, ICMR-National Institute of Malaria Research, Dwarka, New Delhi, 110077 and India.

[2] Academy of Scientific and Innovative Research (AcSIR), Ghaziabad, Uttar Pradesh- 201002.

* Correspondence: rkdixit@icmr.gov.in; cnayadav11@gmail.com

Teaser: Iron imbalance affects reproductive outcome, microbial population, and brain function of the mosquito.

Abstract

Our study investigated how adult female mosquitoes regulate systemic iron homeostasis after blood feeding, a process essential for reproduction, and revealed striking parallels to iron deficiency disorders in mammals. This study shows that a coordinated transcriptional regulation of *Ferritin (Fer)* and *Transferrin (Trf)* plays a crucial role in follicle development and egg maturation. Silencing of both genes using RNA interference (RNAi) led to severe reproductive impairment, including ovarian arrest in 50% of females, 40% reduction in oocyte number, and a decrease in first instar larval size. These outcomes correlate with increased reactive oxygen species (ROS) and altered serotonin receptor (5-HTR) expression in the brain, possibly driven by microbial Gut-Brain-Axis communication alteration due to disrupted iron metabolism. Additionally, we also report the discovery of a previously unknown mosquito gene encoding a hepcidin-like peptide (*AcHep*), expressed in the fat body. This finding reflects the role of mammalian hepcidin, a central regulator of iron homeostasis, suggesting a conserved evolutionary mechanism. In summary, our research provides the first molecular proof and new conceptual understanding that iron metabolism disorders may affect mGBA communication and, in turn, reproductive outcomes.

Keywords: mosquito; blood-feeding; iron homeostasis; microbiome; gut-brain axis

1. Introduction

Iron is a universally essential micronutrient, vital for cellular respiration, DNA synthesis, and oxidative metabolism. In mammals, iron homeostasis is tightly regulated to prevent deficiency or overload, with dysregulation contributing to anemia, sepsis, and neuroinflammation[*1*]. Unlike vertebrates, insects lack hemoglobin-bound iron and instead acquire this metal through dietary sources, including blood meals in hematophagous species such as mosquitoes.

Adult female mosquitoes consume iron-rich blood to initiate vitellogenesis and support oocyte maturation—a process governed by coordinated endocrine and nutrient-responsive pathways(*2–5*). Although the hormonal regulation of vitellogenesis is well characterized, the influence of systemic iron fluctuations on ovarian development and reproductive success remains incompletely understood. Emerging evidence further suggests that nutrient fluctuations, including those associated with blood-derived iron metabolism, can also modulate broader physiological networks

 doi:10.20944/preprints202602.0119.v1

such as the microbiome–gut–brain axis[*6*]. Because adaptation to the blood-feeding is a high-risk, high-reward process, and blood iron serves numerous physiological functions, a multifactor protective mechanism has been proposed to avert oxidative stress in blood-feeding insects[*7*]. This evolutionary specialization to blood-feeding presents a unique opportunity to investigate the potential mechanism by which adult female mosquitoes regulate systemic iron homeostasis, which may be more akin to that of mammals[*8*,*9*].

The cycling of two iron forms, i.e., reduced ferrous (Fe^{2+}) or oxidized ferric (Fe^{3+}) ions, between two distinct oxidation states, is an important aspect of iron homeostasis in any organism[*10*]. Unbound ferrous iron can catalyze the production of harmful free radicals *via* the Fenton reaction, which tightly regulates iron sequestration and trafficking[*11*]. As a result, evolution into a protein-bound state of iron limits its accumulation and harmful chemical effects in a living system[*12*]. In vertebrates, this balance is maintained by proteins such as ferritin (storage), transferrin (transport), and hepcidin (systemic regulation)[*13*]. In hematophagous insects, several studies—particularly those by Oliveira, Oliveira-Paiva, and colleagues have established important roles for ferritin, transferrin, and heme-detoxifying pathways in managing iron from the blood meal[14–*17*]. However, despite this foundational work, the extent to which these proteins interact to coordinate *systemic* iron mobilization across tissues, or how iron flux integrates with reproductive output and microbiome–gut–brain-axis (mGBA) signaling, remains incompletely understood.

A single blood meal (~2-3 microliters), is sufficient to satisfy the iron need for the gonotrophic cycle in mosquitoes. Export mechanisms for heme and ferritin-bound iron are undefined yet; a mechanistic overview suggests that the efflux of ferrous ions follows oxidation to ferric ions, which are then bound to serum transferrin for transportation to other cells[*7*]. The absence of the mammalian homolog *ferroportin,* which exports ferrous ions as a substrate for oxidation *via* ferroxidase, is still an unaddressed problem in mosquitoes[*18*]. Though in the tick *Ixodes ricinus*, silencing of intracellular ferritin (*fer-2*), which also carries a conserved ferroxidase site, and iron-regulatory protein (*irp1*), significantly impairs the reproductive outcome[*19*], but the nature of systemic iron regulation is understudied.

Previously, we have shown that the microbiome–gut–brain axis (mGBA) in *An. culicifacies* integrates metabolic and reproductive signalling in response to blood feeding[*6*]. This process aids in the optimal digestion and distribution of nutrients essential for ovarian growth, primarily through the fat body and hemolymph [*20*]. In another study, we demonstrated that fat-body expressing *transferrin* (*Trf*) plays a major role in iron transportation, and mRNA depletion of this transcript significantly impairs oocyte development in the mosquito *Anopheles culicifacies* [*21*]. But the role of vertebrate's homolog, metalloprotein *ferritin,* in iron homeostasis and reproductive physiology remains unexplored. Given the established interplay between gut microbiota and host iron metabolism in mammals, we hypothesized that iron homeostasis may serve as a regulatory hub linking reproduction, neurophysiology, and microbial balance in mosquitoes (Figure 1).

 doi:10.20944/preprints202602.0119.v1

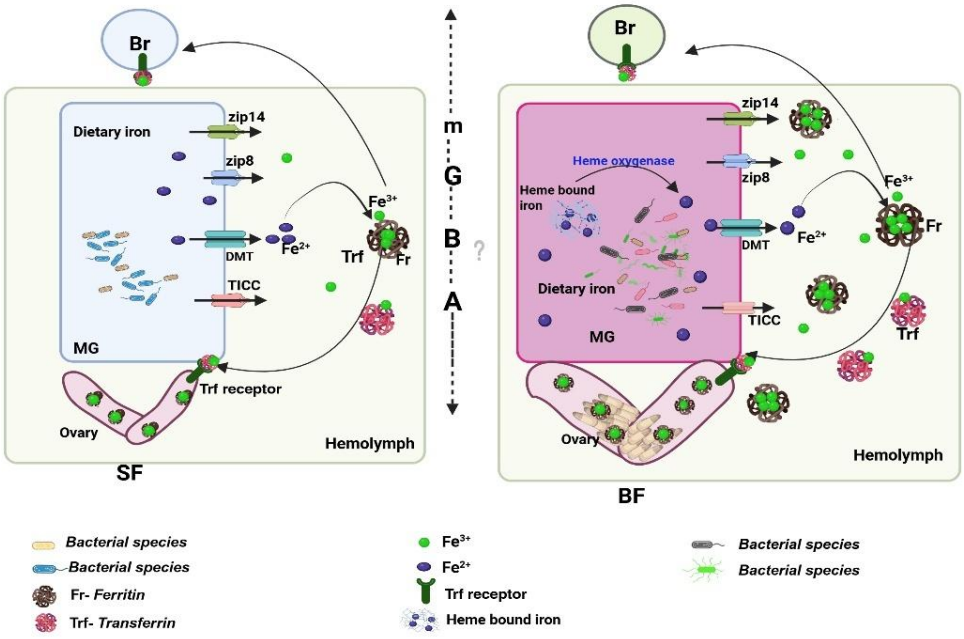

Figure 1. Proposed working hypothesis illustrating the roles of Ferritin and Transferrin in systemic iron regulation in ***Anopheles culicifacies***: Female mosquitoes initially acquire low levels of dietary iron from sugar meals, where free ferrous (Fe^{2+}) iron is absorbed across the midgut epithelium *via* metal transporters such as ZIP family proteins, DMT, and TICC. Within the hemolymph, Ferritin oxidizes Fe^{2+} to ferric iron (Fe^{3+}) for safe storage, while Transferrin transports Fe^{3+} to peripheral tissues, including the brain, through the blood–brain barrier. Following an iron-rich blood meal, both Ferritin and Transferrin are modulated to buffer elevated iron availability and redirect iron toward the fat body and ovaries to support vitellogenesis. The model highlights coordinated, inter-organ iron mobilization across the midgut, hemolymph, fat body, and ovary, illustrating how these proteins maintain systemic iron homeostasis and preserve microbiome–gut–brain-axis (mGBA) balance in gravid females.

To test and evaluate this hypothesis here, we investigated the transcriptional dynamics and physiological functions of ferritin and transferrin in *An. culicifacies*. Using RNAi-mediated knockdown, we uncover their critical and synergistic roles in promoting egg maturation, mitigating oxidative stress, and maintaining neural and microbial homeostasis. Moreover, we report the discovery of a hepcidin-like gene in the mosquito fat body, hinting at an evolutionarily conserved mechanism of systemic iron regulation. Together, our findings illuminate a central role for iron in coordinating mosquito reproductive biology and reveal a new axis of vulnerability that can be exploited for vector control.

2. Methodology

2.1. Mosquito rearing and maintenance

An. culicifacies (sibling species A) was reared and maintained in the ICMR-National Institute of Malaria Research's central insectary facility under conventional rearing conditions of 28 ±2°C temperature, 60-80% relative humidity, and a 12:12 hr light/dark cycle[*6*]. All protocols for the cyclic colony of mosquito rearing and maintenance of the mosquito culture were approved by the ethical committee of the ICMR- National Institute of Malaria Research, New Delhi (NIMR/IAEC/2017-1/07).

2.2. Exogenous ferric chloride feeding assay

A control group (100 mosquitoes) of freshly emerged mosquitoes was given only a 10% sugar solution, whereas test groups (100 mosquito) received sugar with ferric chloride at varying

 doi:10.20944/preprints202602.0119.v1

concentrations (1 mM, 5 mM, and 10 mM). The sugar solution and the supplemented meal were given through cotton swabs and changed after 24 hours with a fresh meal. Survival of the mosquitoes was monitored every 24 hours of iron supplementation. Haemolymph, fat body, midgut, and ovary were collected from surviving 20–25 mosquitoes from each set (control and supplemented test group) after 72hr of supplementation to assess the transcriptional response of target transcripts.

2.3. Mosquito tissue sample collection:

As per the experimental design, the desired tissues were collected from 4-day-old *An. culicifacies* mosquitoes to evaluate spatial-temporal expression. For this purpose, ice-anesthetized mosquitoes (20 mosquitoes) were placed on a slide under the dissecting microscope one by one, and dissected with the help of a sharp needle. Different tissues including the salivary gland, midgut, fat-body, hemolymph, and female reproductive organ was dissected and collected in Trizol reagent as described previously[*21*]. The aquatic development stages, such as egg, larvae, and pupa of the *An. culicifacies* were also collected in Trizol reagent. To explore the fate of iron, we focused on relevant tissues such as the haemolymph, fat-body, mid-gut, and ovary collected from both naive sugar-fed and blood-fed mosquitoes of the same cohort at pre-defined time intervals.

Initially, targeted tissues were collected from sugar-fed mosquitoes aged 3- 4 days, while to meet the blood-fed condition, a live and healthy rabbit was placed inside a mosquito cage for blood-feeding. Then selected tissues were collected from a fully engorged female mosquito at 0-2 hours, 24 hours, 48 hours, and 72 hours after the blood meal for detailed tissue-specific gene expression analysis. For hemolymph collection, an anticoagulant solution containing (60% Schneider's medium, 10% fetal bovine serum, and 30% citrate buffer) was injected into the thorax, and a small incision was made near the posterior two segments of the distended belly with a minuscule needle, allowing translucent hemolymph to ooze out. Using a micropipette, hemolymph was taken and pooled in Trizol. Fat-body was recovered by extracting all abdominal tissues from the last two abdominal segments and then forcibly tapping the abdominal carcass till pale yellow fat-body oozed out.

2.4. Total RNA isolation and cDNA synthesis

Total RNA was isolated from collected samples manually by Trizol method, as previously described[*40*]. Isolated RNA was quantified with the help of a Nanodrop 2000 spectrophotometer (Thermo Scientific, USA), and ~1 µg of total RNA was used for the synthesis of the first-strand cDNA using the cDNA synthesis kit (PrimeScript™ 1st strand cDNA Synthesis Kit, Cat. # 6110A, Takara). Actin was used as a reference gene in RT-PCR to evaluate the quality of the cDNA.

2.5. Gene expression analysis through Quantitative PCR

For gene expression analysis, a real-time PCR-based transcriptional profiling assay was performed using the Sybr Green qPCR Mastermix (Takara, TB Green Premix Ex Taq™ II, Cat# RR820A) and CFX 96 Real-Time PCR system (C1000 Touch Thermal Cycler, Bio-Rad, USA). Three independent biological replicates were run under the identical PCR conditions, starting with denaturation at 95°C for 5 min, 40 cycles of 10 sec at 95°C, 15 sec at 52°C, and 22 sec at 72°C. Each cycle's fluorescence reading was recorded at 72°C after it had finished. For determining a melting curve, the final PCR stages at 95°C for 15 sec, 55°C for 15 sec, and again 95°C for 15 sec were accomplished. Throughout the study, the Actin and Rps7 genes served as reliable internal control (reference gene), which were found with stable expression throughout different stages and tissues of the mosquito[*41*]. The relative quantification was examined using the $2^{-\Delta\Delta}$Ct method.

2.6. dsRNA-mediated gene knockdown assays in adult mosquitoes

A double-stranded RNA-mediated gene knockdown assay was executed to suppress target gene mRNA expression. Single-stranded cDNA was first amplified using a dsRNA primer (Primer sequence provided in Table S6) with a T-7 overhang primer as listed in the Supplemental Table 6.

 doi:10.20944/preprints202602.0119.v1

Following amplification, the PCR product was purified through a Gene Jet purification kit (Thermo Scientific, Gene JET PCR Purification Kit, Cat #K0701) and quantified by Nano-drop 2000 spectrophotometer (ThermoScientific, USA). Using the transcript aid T-7 high yield transcription kit (Cat# K044, Ambion, USA), dsRNA was in-vitro synthesized by employing the purified PCR product as a template. The resulting reaction product was again purified, quantified, and approximately 69 nl (~3ug/ul) was injected into the thoracic region of a 1-2 day old cold-anesthetized mosquito using a nano-injector (Drummond Scientific, USA, Cat# 13681455). Concurrently, for the negative control group, dsRNA of bacterial-GFP was injected into the mosquitoes of the same cohort. After 48 hours of post-injection, tissue samples were dissected from both the gene-specific i.e. Ferritin only, and in combination with Transferrin (Trf), as well as control (GFP-injected) injected mosquitoes. To determine the silencing effectiveness, a real-time PCR-based assay was performed as described above.

2.7. Assessment of ovary development following gene silencing

Both the control (GFP dsRNA-injected) and experimental (*Fer* + *Trf* dsRNA-injected) mosquito groups were fed on the rabbit, after 48 hours of post-injection and only fully fed mosquitoes were selected for the evaluation of ovary development, while partially fed or unfed mosquitoes were excluded. To evaluate ovary growth, anaesthetized mosquitoes were placed on dissecting slides under a binocular stereomicroscope and detached ovaries in phosphate-buffered saline (PBS) at 72 hours post blood feeding. The mature oocytes inside the ovaries were manually counted, and the results were compared to control mosquitoes. However, gradual follicular development was compared within naïve sugar-fed, 24 hr, 48 hr, and 72 hr blood-fed mosquito ovaries. Dissected ovaries from anesthetized mosquitoes were treated with PBS-T (Phosphate Buffered Saline with 0.5% Triton X-100) solution for 2-3 minutes, followed by thorough washing with 1X PBS. The samples were then incubated for 5 min. with DAPI (4,6-diamidino-2-phenylindole, 300 nM). After staining, extra stain was removed by washing three times with 1X PBS in the dark, and tissue was imaged at excitation/emission: 358 nm/461 nm under a Leica confocal microscope (Thermo-fisher, USA)[*42*,*43*].

2.8. Metagenomic profiling

For WGS-metagenomic analysis, we collected gut samples from 24 hours of blood-fed control and *Fer+Trf* KD adult female mosquitoes. Before dissection, the body surface of the mosquitoes was sterilized using 70% ethanol for 1 min. (5 mosquitoes per batch), followed by aeration on a sterilized filter paper. The gut dissection was carried out in 1X PBS, under the laminar flow, where the working area as well as the dissecting stereomicroscope were kept sterilized by using 70% ethanol. We followed a sample pooling strategy, which provides a reliable and comprehensive overview of the gut-bacterial community structure, if aimed at comparing within similar samples(*6*,*44*). For the purpose, pooled guts (50 whole midguts) were collected into a minimal volume (100ul) of sterile ice-cold 1X PBS and outsourced for WGS sequencing. High-quality genomic DNA was extracted from the collected sample. After isolation, it was quantified and evaluated for quality and integrity. Library construction included appropriate adaptor ligation with DNA fragments, followed by amplification and sequence alignment (https://biologyinsights.com). The raw fastq reads were pre-processed using Fastp v.0.20.1(parameters: --length_required 50 --qualified_quality_phred 30 -- unqualified_percent_limit 30 --average_qual 30)[*45*]. Read-level taxonomic profiling was done by aligning the processed paired-end reads to the pre-KMA-indexed NCBI 2019 Genome Build (http://dx.doi.org/10.25910/5cc7cd40fca8e) database using KMA[*46*]. The resulting KMA files were subjected to metagenomic profiling using CCmetagen v.1.2.5 and visualized using krona (CCMetagen-1.2/)[*47*] and stacked bar plots were plotted using phyloseq R-packages[*48*].

 doi:10.20944/preprints202602.0119.v1

2.9. Oxidative stress measurement assays

To assess the impact of iron homeostasis disruption on oxidative stress-mediated alteration in the midgut and brain, we performed molecular, biochemical, as well as cellular assays as described below.

2.9.1. Molecular assay

Brains from control and *Fer+Trf* knockdown mosquitoes (n = 15 per group) were dissected 48 h after dsRNA injection to evaluate the expression of oxidative stress–associated genes. Total RNA was isolated from pooled brain tissues, followed by cDNA synthesis and quantitative real-time PCR analysis of *NOS* expression in naïve sugar-fed mosquitoes, as described above. For the assessment of *SOD* expression, a separate cohort of control and knockdown mosquitoes was provided a blood meal 72 h after dsRNA injection. Midguts were dissected 24 h post-blood feeding, and *SOD* transcript levels were quantified using qPCR following the same RNA extraction and cDNA preparation workflow.

2.9.2. Cellular Assay

Oxidative stress in naïve sugar-fed (SF), blood-fed (BF) control, and *Fer+ Trf* KD mosquito groups, was evaluate through ROS assay. Dissected brain tissue from 15 mosquitoes of each group were incubated with an oxidant-sensitive fluorophore dye CM- H2DCFDA[5-(and-6)-chloromethyl-29,79-dichloro-dichlorofluorescein diacetate, acetyl ester, 2mM] (Sigma, St. Louis, MO, USA), for 20 min at room temperature under dark conditions. To remove the extra staining, tissue was washed thrice with 1X PBS and observed under a Leica confocal microscope, observing at excitation/emission: 480nm/530nm to detect ROS accumulation *[43].*

2.9.3. Biochemical Assay

Alternatively, to estimate the oxidative stress, we collected 15 mosquitoes' brains in 1X PBS, and then briefly centrifuged to extract the supernatant for nitrite quantification using the Griess Reagent Kit (Cat. # G792,Thermo Fisher Scientific, USA). N-(1-aphthyl) ethylenediamine dihydrochloride(Component A) and Sulfanilic acid (Component B), were mixed, followed by the addition of 130 µL of the mixture, 20 µL of deionized water, and 150ul of the test sample as per kit manual. The final mixture was loaded in a 96-well U-shaped ELISA plate and incubated in the dark for 30 minutes. While 20 µL of Griess Reagent and 280 µL of deionized water mixture were considered as a reference sample, which was also loaded onto a plate, and absorbance was recorded at 548 nm using an ELISA Reader (Tecan Unlimited M200pro Instrument)[*49*].

2.10. Statistical analysis

For statistical analysis, test sample data were compared with the control data set using GraphPad Prism software, and treatment differences were determined through a one-way ANOVA test for multiple comparison with respective control with the help of Dunnett's multiple comparisons post-hoc test. For pairwise group comparison (control vs knockdown), an unpaired two-tailed Student's *t*-test was applied. Statistical significance was established at $p < 0.05$ in addition with 95% CI (confidence interval) for mean differences were calculated to provide an estimate of effect size and the precision of the observed differences. For survival analysis, mortality and survival data of mosquitoes after iron supplementation were analysed using the Kaplan–Meier method, and survival curves were compared using the Log-rank (Mantel–Cox) test. Hazard ratios with 95% confidence intervals (CI) were calculated to assess the relative risk of mortality between control and treated groups. All experiments were conducted thrice for data validation.

 doi:10.20944/preprints202602.0119.v1

3. Result

3.1. Ferritin and Transferrin are co-regulated for iron mobilization in egg development

Our structural and functional prediction analysis, verifying iron-binding properties (Figure S1), suggested that mosquitoes' *transferrin* and *ferritin* may have a similar role in systemic iron homeostasis and reproductive physiology, as in mammals. Structure prediction and modelling analysis showed that *Trf* and *Fer* proteins carry distinct functional domains to bind iron. Further, to explore the dynamics of systemic iron regulation, we first characterized the spatial and temporal expression of ferritin (*Fer*) and evaluated the possible correlation with transferrin (*Trf*). Much like transferrin *[21]*, we found that *Ferritin* is dominantly expressed in eggs and pupae among aquatic developmental stages, and in adult females than in age-matched male mosquitoes (Figure 2A), which records a distinct instance of adaptive evolutionary benefits to feed on an iron-rich blood meal and procreate.

Tissue-specific analysis further showed that *Fer* is enriched in the hemolymph and reproductive tissue (Figure 2B; Figure S2A), while *Trf* predominantly localizes to the fat body in the naïve sugar-fed mosquito *[21]*, indicating coordinated but compartmentalized roles. Following blood feeding, *Fer* expression surged in the midgut (Figure 2C) and fat body (Figure 2D) at 24 hours post-meal, gradually returning to baseline by 72 hours post-meal. In contrast, ovarian (Figure 2E) and hemolymph (Figure 2F) *Fer* expression steadily increased over 72 hours, suggesting its role in iron provisioning during vitellogenesis, a biphasic expression pattern observed for *Trf* [*21*]. Notably, expression of heme oxygenase, a heme-degrading enzyme, was also induced at 24hr after blood feeding in the midgut of blood-fed mosquito (Figure S2B), supporting active iron release in the midgut [*22*]. Collectively, these findings suggest a spatiotemporal coordination is essential between *Fer* and *Trf* across the gut, fat body, ovary, and hemolymph to facilitate iron trafficking during oocyte development.

 doi:10.20944/preprints202602.0119.v1

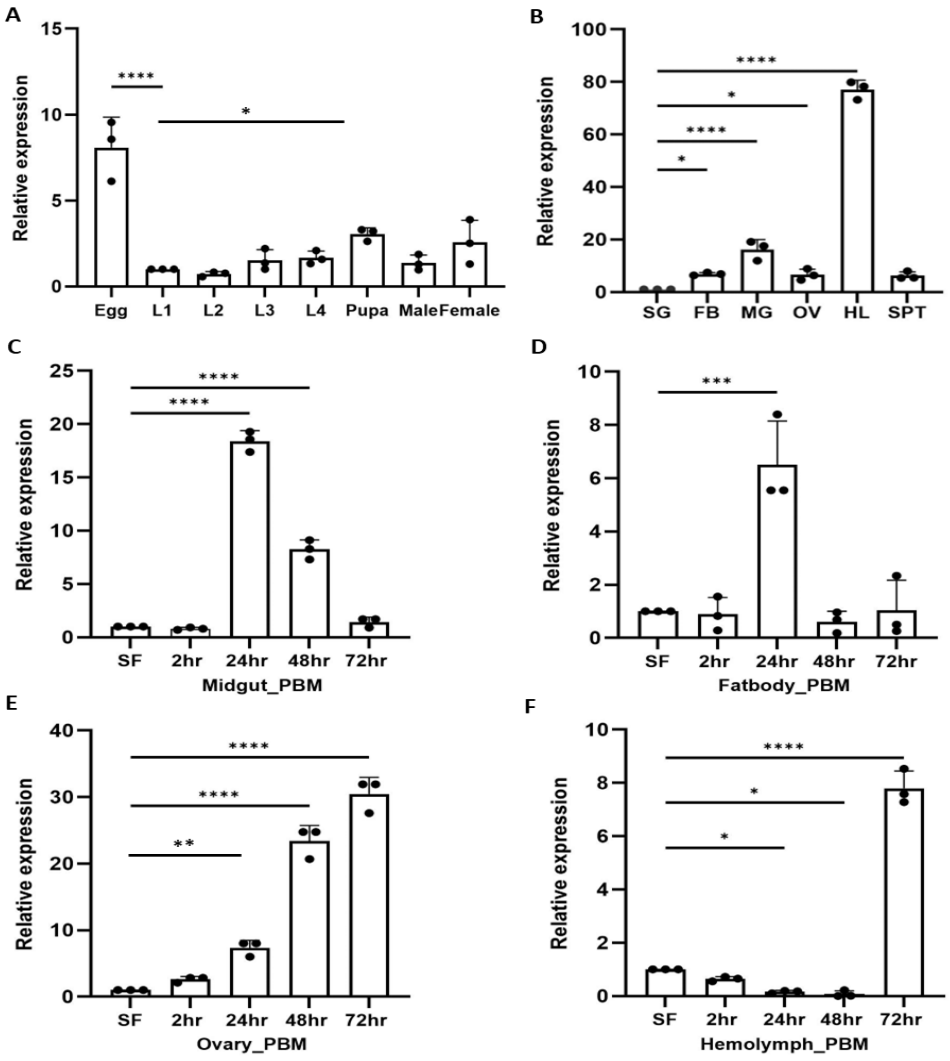

Figure 2. Spatio-temporal regulation of *ferritin* (*Fer*) expression supports iron mobilization in female mosquitoes: (A) Relative expression of *Ferritin* (ACUA006714) during aquatic development, showing increased expression of *Fer* in the egg (p<0.0001), and pupa (p<0.0451) of the mosquito. Here, the first instar larva was considered as a control for all test samples. (N=3, n=10). **(B)** Tissue-specific expression analysis in naïve adult female mosquitoes showing high abundance in hemolymph (p<0.0001), midgut (p<0.0001), fat-body (p<0.0373), ovary (p<0.0483), and spermatheca in decreasing order, considering salivary gland as a control for all test samples. (N=3, n=25). **(C-F) Temporal dynamics of ferritin expression following blood feeding (PBM) (C) Midgut (**MG), increased expression at 24hr (p<0.0001), and 48hr (p<0.0001) PBM; **(D) Fat Body** (FB), up-regulated expression at 24hr PBM (p<0.0001); **(E) Ovary (**OV): Progressive increase at 24hr (p<0.0025), 48hr (p<0.0001) and 72hr (p<0.0001) PBM; **(F) Hemolymph (**HL), peak induction at 72hr PBM (p<0.0001). All the post-blood meal expression assays were performed across three independent biological replicates, and sugar-fed female tissues were considered as a control for all test samples. All qPCR data were analyzed using one-way ANOVA with Dunnett's multiple comparison test. Significance levels: *p < 0.05; **p < 0.005; ***p < 0.0005. (N = number of biological replicates, n=number of mosquitoes dissected for sample collection). Here, SG- Salivary gland, FB- fat body, MG- Midgut, OV-Ovary, HL- Hemolymph, SPT- Spermatheca, PBM- Post blood meal.

3.2. Exogenous iron elevates ferritin expression and affects mosquito survival

To examine whether iron supplementation perturbs iron homeostasis, we exposed sugar-fed female mosquitoes to increasing concentrations of ferric chloride. At 1 mM, survival was comparable to that of the control; however, concentrations of 5–10 mM significantly reduced lifespan (Figure S2C). Ferritin expression in the hemolymph increased proportionally with iron dose (Figure S2D), whereas ovarian expression remained static after 1mM (Figure S2E). This pattern suggests an

 doi:10.20944/preprints202602.0119.v1

enhanced iron-sequestration response in the hemolymph, consistent with the established roles of ferritin and transferrin in buffering and redistributing excess dietary iron in insects. Notably, earlier studies have shown that 1 mM iron supplementation induces Transferrin expression in the fat body and enhances oocyte number[21], further supporting a coordinated regulatory response to elevated iron availability. Though, higher iron concentrations (5–10 mM) were associated with decreased survival, but additional physiological measurements are needed to determine the specific mechanism underlying this reduction.

3.3. Dual knockdown of Fer and Trf impairs reproduction

To dissect the functional contribution of Ferritin (Fer) and Transferrin (Trf) to reproductive physiology, we first performed RNAi-mediated silencing individually and in combination. Silencing of *Fer* alone led to at least 90%, 60%, and 50% reduction of *Fer* transcript in the hemolymph, fat body, and midgut of the injected mosquito group (Figure 3A), respectively, and triggered a compensatory upregulation of Trf in the hemolymph (Figure 3B), accompanied by a significant decline in mature oocyte numbers (Figure 3C). This compensatory response suggests that the mosquito attempts to preserve iron transport capacity when iron-storage ability is compromised (Figure S2F).

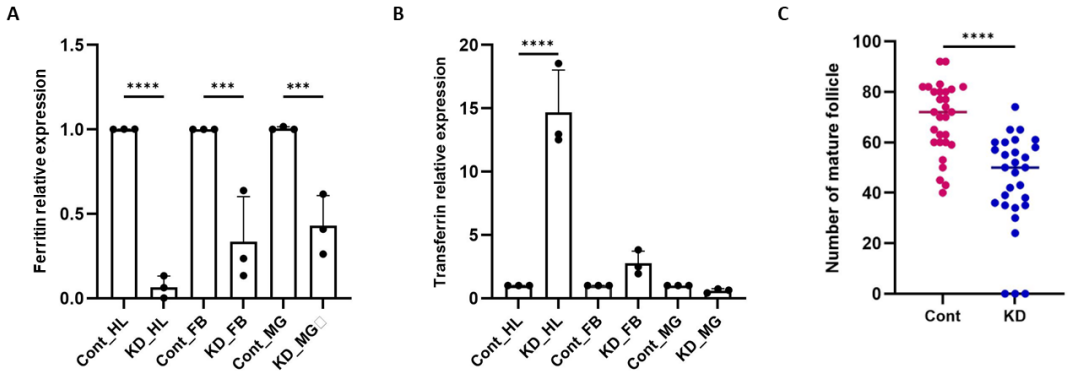

Figure 3. Ferritin knockdown impairs ovarian maturation and modulates transferrin expression: (A) qPCR analysis of Ferritin (Fer) knockdown efficiency in 1–2-day-old females injected with dsFer, using dsGFP-injected mosquitoes as controls. Fer transcript levels were significantly reduced in hemolymph (HL; $p < 0.0001$), fat body (FB; $p < 0.0002$), and midgut (MG; $p < 0.0006$) (N = 3, n = 25). Data were analyzed using one-way ANOVA with Šídák's multiple comparisons test (Control *vs*. Knockdown for each tissue). **B)** Transferrin (Trf) expression following Ferritin silencing: A significant upregulation of *Trf* was observed in hemolymph ($p<0.0001$), while changes in fat body ($p<0.4021$) and midgut ($p<0.9823$) were not significant (N = 3, n = 25). Statistical analyses were performed using one-way ANOVA with Šídák's multiple comparisons test. Significance levels: *p < 0.05; **p < 0.005; ***p < 0.0005. **(C)** Impact of Ferritin knockdown on ovarian maturation: Dot-plot analysis revealed a significant reduction in the number of mature follicles in dsFer-injected females compared with dsGFP controls ($p<0.0001$) (N = 3, n = 10). Each dot represents the number of mature follicles per female. Data were analyzed using an unpaired two-tailed Student's t-test. (N = number of biological replicates, n= number of mosquitoes dissected for sample collection). MG-Midgut, FB-Fat-body, HL- Hemolymph, Cont.- Control, KD- Knockdown.

Strikingly, co-silencing of *Fer* and *Trf* resulted in decreased expression of *Fer* and *Trf* to 50% and 70% respectively in hemolymph (Figure 4A). In stark contrast, dual-silenced mosquitoes elicited a markedly more severe phenotype: approximately ~40% reduction in oocyte number (Figure 4B), and 50% of females exhibited complete ovarian arrest (Figure S3A-C, Table S1). These defects illustrate the non-redundant and cooperative roles of *Fer* and *Trf* in enabling iron mobilization for oogenesis.

Egg and larval progeny (first instar larvae) of *Fer+Trf* knockdown females further showed a significant reduction in body size and delayed early developmental progression (Figure S3D; Figure 4C–D, Table S2), consistent with impaired maternal iron provisioning during embryogenesis. Microscopic assessment of follicle development revealed disorganized ovarian architecture in

 doi:10.20944/preprints202602.0119.v1

double-knockdown females, with many follicles failing to progress beyond early vitellogenic stages, indicating that the depletion of both iron-binding proteins severely restricts the availability of iron-dependent enzymatic processes required for vitellogenin maturation and proper chorion biogenesis (Figure 4E). Together, these results show that dual silencing destabilizes the inter-organ iron-regulation network essential for the gonotrophic cycle, while Ferritin and Transferrin jointly safeguard systemic iron flow required for normal ovarian development and offspring viability.

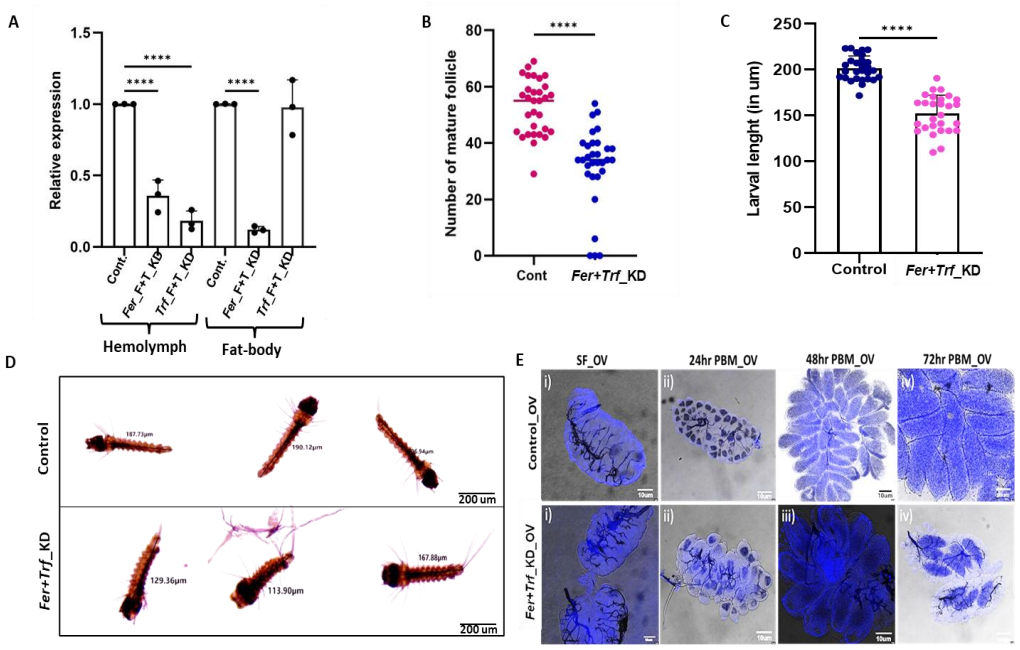

Figure 4. | Dual knockdown of *Ferritin* and *Transferrin* disrupts ovarian maturation and reduces offspring size: (A) qPCR validation of simultaneous knockdown of *Ferritin* (Fer) and *Transferrin* (Trf) in hemolymph (HL) and fat body (FB) of 2-day-old *dsFer+dsTrf*–injected females, showing significant transcript reduction relative to *dsGFP* controls ($p < 0.0001$ for both tissues). Values represent three biological replicates (N = 3, n = 25). Statistical significance was assessed using one-way ANOVA followed by Šídák's multiple-comparison test (*p < 0.05; **p < 0.005; ***p < 0.0005); **(B)** Mature ovarian follicle counts demonstrating a marked reduction in follicle number in *dsFer+dsTrf* females compared with controls (N = 3, n = 10 per group). Each dot represents a single ovary pair. Significance determined using an unpaired two-tailed Student's t-test; **(C)** Larval body-size measurements showing significantly smaller first-instar larvae derived from dsFer+dsTrf females relative to control progeny (N = 3, n = 9). Data analyzed using an unpaired Student's t-test (*p < 0.05; **p < 0.005; ***p < 0.0005); **(D)** Representative micrographs of first-instar larvae from control and double-knockdown females illustrating the reduction in larval length following *Fer+Trf* silencing. Images were captured at 4× magnification using a camera-mounted microscope (scale bar = 200 µm), and the size was measured individually through the in-built program available in the image processing software of the camera **(E).** Comparative ovarian development following *Fer+Trf* knockdown. Representative DAPI-stained ovaries from control and *Fer+Trf* Knockdown females under sugar-fed and blood-fed conditions: ***(i)*** Sugar-fed controls exhibit compact early-stage follicles with uniform nuclear staining, whereas *Fer+Trf* KD ovaries display smaller, poorly organized follicles with reduced nuclear density; ***(ii)*** 24 h PBM controls show normal initiation of vitellogenesis with enlarged, well-organized follicles. In contrast, 24 h PBM *Fer+Trf* KD ovaries exhibit delayed follicle expansion and irregular nuclear distribution; ***(iii)*** 48 h PBM controls reach advanced vitellogenic stages with tightly packed follicles; KD ovaries remain developmentally delayed, with flattened or irregularly shaped follicles and disrupted epithelial organization; ***(iv)*** 72 h PBM controls display fully matured, elongated ovarioles typical of late vitellogenesis, while KD ovaries show clear follicular arrest, incomplete growth, and failure to attain terminal maturation stages.

All ovaries were dissected, stained with DAPI for 5 min, washed, and imaged using a Leica confocal microscope. Scale bars = 10 µm. (N = number of biological replicates; n = number of ovaries

 doi:10.20944/preprints202602.0119.v1

analyzed per group.) Fer – Ferritin; Trf – Transferrin; HL – Hemolymph; FB – Fat body; PBM – Post-blood meal.

3.4. Iron disruption reshapes gut microbiota composition and function

Given the known links between iron and microbial ecology(*23–25*), we profiled gut microbiota by whole-genome shotgun sequencing. Knockdown of *Fer+Trf* significantly altered bacterial composition, reducing the abundance of iron-sensitive taxa such as *Aeromonas hydrophila*, *Enterobacter hormaechei*, and *Klebsiella aerogenes*, while enriching *Klebsiella pneumoniae* and *Enterobacter asburiae* (Figure 5A; Figure S4A–D). Functional pathway analysis revealed differential enrichment of enzymes related to iron acquisition, redox balance, and metabolic turnover (Figure 5B; Figure S4E; Table S3), suggesting microbial adaptation to altered host iron status. These results demonstrate that systemic iron perturbation drives gut microbial dysbiosis, reinforcing the role of iron as a modulator of mGBA integrity[*26*,*27*].

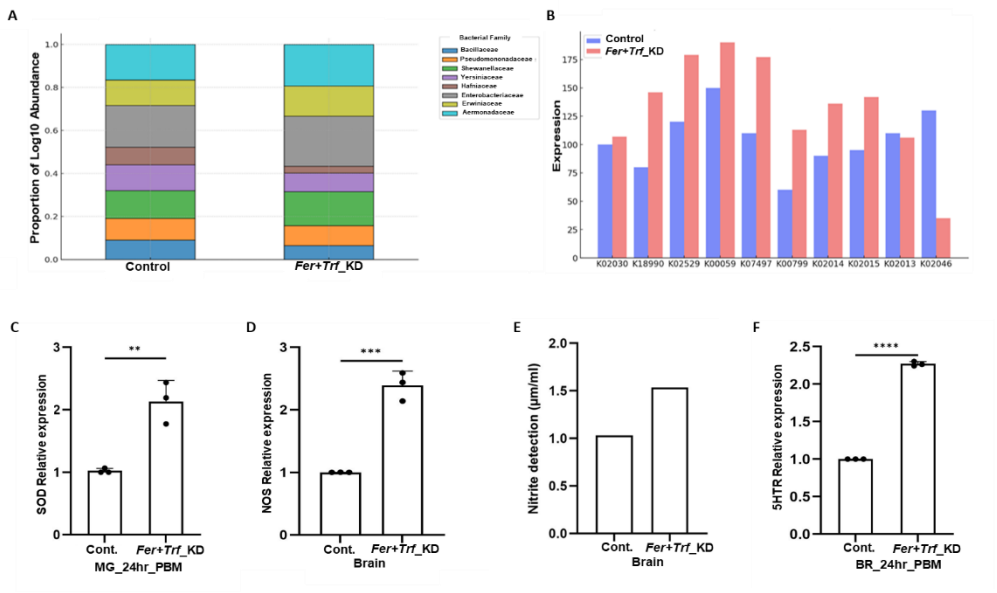

Figure 5. Iron homeostasis disruption alters gut microbiota composition and oxidative stress responses in brain: (A) Taxonomic abundance shifts in gut microbiota (Kraken2 analysis): Stacked bar charts display bacterial family-level abundance in Control *vs*. *Fer+Trf* KD samples based on Kraken2 classification. The Y-axis represents log_{10}-transformed relative abundance, with color-coded bacterial families illustrating KD-induced microbiota restructuring. **(B)** Predicted microbial gene expression changes (KMA-based analysis): Bar charts represent differences in predicted metabolic pathway–linked gene expression between Control and *Fer+Trf* KD samples. Processed paired-end reads were aligned to the NCBI 2019 Genome Build using KMA. Red bars indicate *Fer+Trf* KD samples; blue bars indicate Controls. Expression shifts suggest substantial metabolic reprogramming of the microbiota following dual knockdown. **(C)** Relative gene expression analysis of *SOD* in midguts of 24hr blood-fed double knockdown (*Fer+Trf* KD) females shows significantly elevated *SOD* expression ($p < 0.0024$) compared with age-matched dsGFP controls (N = 3, n = 25). Data were analyzed using an unpaired two-tailed Student's *t*-test (*p < 0.05; **p < 0.005; ***p < 0.0005). **(D)** Real-time expression analysis of *NOS* in brains of *Fer+Trf* KD mosquitoes demonstrates strong induction of *NOS* (p < 0.0001) relative to dsGFP controls (N = 3, n = 25). **(E)** Nitrite accumulation in the mosquito brain following iron homeostasis disruption. Relative nitrite levels were quantified in control and *Fer+Trf* KD females, showing elevated nitrite levels in KD samples. **(F)** Expression of *5HTR* in the brains of 24hr blood-fed *Fer+Trf* KD females shows significant upregulation ($p < 0.0001$) compared with dsGFP controls (N = 3, n = 25). Statistical analysis was performed using an unpaired two-tailed Student's *t*-test (*p < 0.05; **p < 0.005; ***p < 0.0005). (N = number of biological replicates, n= number of mosquitoes dissected for sample collection). Here, Fer- Ferritin, Trf- Transferrin, HL- Hemolymph, FB- Fat body, PBM-Post blood meal.

 doi:10.20944/preprints202602.0119.v1

3.5. Disruption of iron homeostasis elevates oxidative stress and alters brain signaling

To evaluate whether disrupted iron trafficking triggers oxidative stress, we first assessed antioxidant responses in the gut. Superoxide dismutase (SOD) expression was significantly elevated in the gut of Fer+Trf knockdown mosquitoes (Figure 5C), suggesting increased generation of free radicals, likely driven by excess unbound ferrous iron participating in Fenton reactions [8]. In the mosquito brain, oxidative burden was further reflected by a ~2.5-fold increase in nitric oxide synthase (NOS) transcript levels (Figure 5D), and elevated nitrite levels (Figure 5E), together indicating activation of neuroinflammatory pathways [28,29]. As supportive evidence, DCFDA-based fluorescence measurements further showed higher signal intensity in Fer+Trf knockdown mosquito brains compared with controls (Figure S5A-D). Notably, while control mosquitoes displayed a characteristic transient induction of NOS after blood feeding, NOS expression remained unresponsive in the brain of the knockdown female mosquitoes (Figure S5E-F), suggesting impaired neuro-modulatory adaptation to the blood meal. Moreover, a remarkable induction of 5-HTR (serotonin receptor) expression in Fer+Trf knockdown females after 24hrs of blood-feeding (Figure 5F, Figure S5G) highlighted that iron imbalance disrupts redox equilibrium and perturbs neurochemical signaling, likely through altered Microbiome-Gut-Brain-Axis (mGBA) communication.

3.6. A mosquito hepcidin-like gene suggests conserved iron regulation

From a surprising discovery of three novel transcripts encoding fish homologs Hepcidin, Ceruloplasmin, and Transferrin (Table S4), possibly a result of horizontal gene transfers (Unpublished), we further characterized the gene encoding a small peptide with homology to vertebrate hepcidin (Table S5), here named *AcHep*. Sequence analysis of a 222bp transcript encoding a 59-amino acid-long peptide showed maximum homologies with bony fish and mammals, but failed to show any identity to any insect/mosquito hepcidin orthologs (Figure 6A–D; Figure S6A,B,D). Relative expression profiling confirmed detectable expression of *AcHep* in the fat body of *Fer+Trf* knockdown mosquitoes (Figure 6E; Figure S6C,E). Given the central role of hepcidin in vertebrate iron regulation, this finding suggests the presence of a cryptic, possibly functional, hepcidin analog in mosquitoes. Its induction under disrupted iron conditions further supports a conserved regulatory role.

 doi:10.20944/preprints202602.0119.v1

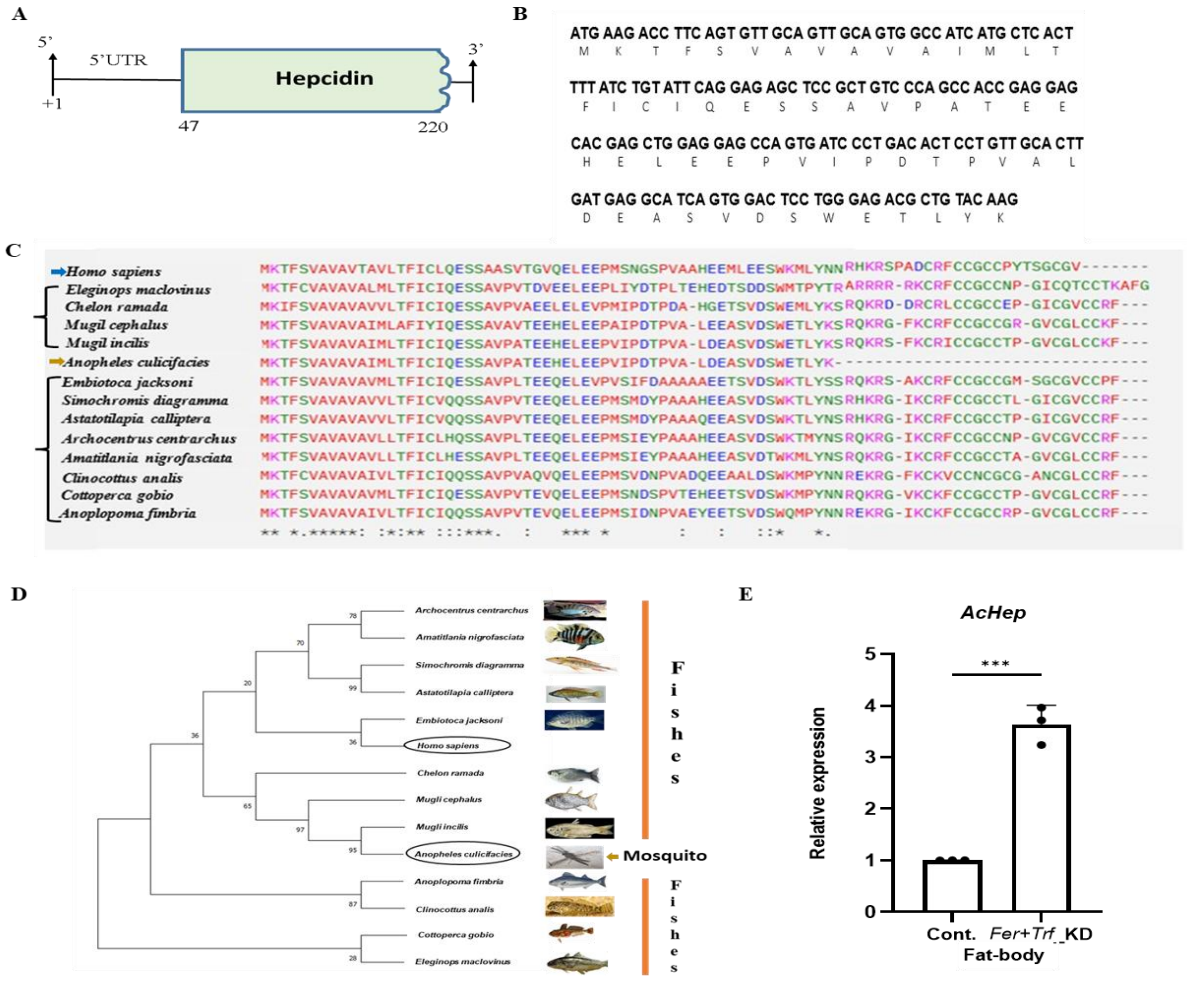

Figure 6. Identification and iron-responsive regulation of a hepcidin-like transcript in *Anopheles culicifacies* **:(A-B)** Genomic organization and molecular features of the partial *An. culicifacies* hepcidin-like cDNA sequence. The identified sequence spans 222 bp and encodes a 59-amino-acid peptide; the coding region is highlighted in green. **(C)** Multiple sequence alignment of the predicted hepcidin-like peptide with homologous sequences from representative species, performed using Clustal Omega. Alignment reveals low similarity with insect sequences but notable homology with vertebrate hepcidins, including *Homo sapiens*. Symbols indicate conservation: "*" fully conserved, ":" strongly conserved, "." weakly conserved positions, and "–" alignment gaps. **(D)** Phylogenetic analysis of the hepcidin-like peptide constructed using MEGA (maximum likelihood method, JTT substitution model, 1000 bootstrap replicates). The *An. culicifacies* sequence clusters closer to vertebrate hepcidins than to insect counterparts. **(E)** Real time transcriptional expression of *AcHep* in fatbody of control and *Fer+Trf* KD mosquito shows significant upregulation ($p < 0.0002$) compared with dsGFP controls (N = 3, n = 25). Statistical analysis was performed using an unpaired two-tailed Student's *t*-test (*p < 0.05; **p < 0.005; ***p < 0.0005). (N = number of biological replicates, n= number of mosquitoes dissected for sample collection).

4. Discussion

Our study demonstrates that *Anopheles culicifacies* mosquitoes deploy a coordinated iron-regulatory system involving ferritin and transferrin to balance this trade-off following a blood meal. Disruption of this regulation impairs reproductive success, alters the gut microbiota, induces oxidative stress, and perturbs brain signaling—collectively suggesting that iron homeostasis is a central node in mosquito physiology.

After the blood meal acquisition, mosquitoes experience a physiological shift that activates multiple organs to synchronize digestion and reproduction[*30*]. During the digestion process, the iron is transported to haemolymph, either for storage in the fat body or mobilized to facilitate ovarian development. While testing this proposition, we found that both ferritin and transferrin exhibit

 doi:10.20944/preprints202602.0119.v1

temporally and spatially regulated expression post-blood feeding, suggesting a biphasic model of iron acquisition and distribution. Functional silencing of both genes not only arrests follicle development but also reduces egg output and compromises larval fitness, highlighting their role in reproductive investment. The observed phenotypes parallel iron-deficiency-related reproductive disorders in mammals, suggesting evolutionary conservation in iron-dependent fertility regulation.

Emerging mammalian studies further highlight the gut microbiota association with iron deficiency-induced anaemia (IDA), which may have a significant influence on the absorption of dietary iron [*31*–*32*], although the exact mechanism is still unknown. Alternatively, in mosquitoes, a bidirectional microbiome-gut-brain-axis (mGBA) communication is found crucial for maintaining the physiological equilibrium and reproductive outcomes[*6*], but its influence on iron regulation remains undetermined. Integrating with current knowledge, our metagenomic profiling data endorses that iron homeostasis disruption reshapes the gut microbiota, selectively reducing taxa associated with iron acquisition and redox balance. These changes in microbial composition and predicted functional pathways suggest a dynamic interplay between host iron regulation and microbial ecology—paralleling gut-microbiome interactions implicated in iron-deficiency anemia in humans[*32*]. Supporting further, we also observed a notable elevation of ROS levels and increased nitric oxide synthase (NOS) activity in the mosquito brain, along with altered expression of serotonin receptors.

Previous research on the hematophagous bug *Rhodnius prolixus* demonstrates that blood feeding instantly raises 5-HTR level, which then gradually declines with completion of post-blood meal digestion[*33*]. In mosquitoes, it contributes to gut-microbial interaction, parasite transmission, and ovarian development[*34*,*35*]. In mammals, iron deficiency correlated with the expression of 5-HT receptor and serotonin level, which trigger multiple neurotransmission activities, including neuro-behavioural manifestations, neuropsychological disorders, and depression[*35*,*36*]. Taken together, our findings indicate that iron status influences neurochemical signalling pathways known to modulate feeding, reproduction, and behavioral disorders *via* altered serotonin pathways[*37*].

Finally, the identification of a hepcidin-like gene (*AcHep*) expressed in the mosquito fat body, the insect equivalent of the mammalian liver, raises the possibility of a conserved iron-regulatory hormone across distant taxa. Hormone hepcidin, which regulates iron homeostasis *via* iron efflux transporter ferroportin, is a well-characterized clinical biomarker for systemic Iron level diagnosis in mammals[*38*,*39*]. Although functionally uncharacterized, *AcHep* may represent a critical missing link in our understanding of insect systemic iron homeostasis.

Together, our findings establish iron homeostasis as a mechanistic bridge between nutrition, neurobiology, microbiota, and reproduction, mirroring the effects observed in mammalian iron deficiency. This work provides a new conceptual framework for understanding the integration of physiological systems in disease vectors and opens novel avenues for targeting iron metabolism as a strategy for mosquito population control.

5. Conclusion

Our findings demonstrate that Ferritin and Transferrin form a cooperative iron-regulatory axis that integrates reproductive physiology, oxidative stress responses, microbial balance, and neurochemical signalling in *Anopheles culicifacies*. Disrupting this axis leads to impaired follicle maturation, reduced offspring fitness, elevated oxidative stress, and altered serotonin-mediated brain signalling, highlighting iron homeostasis as a central determinant of mosquito reproductive success and mGBA function. The identification of a hepcidin-like transcript further suggests that additional, previously unrecognized layers of systemic iron regulation may exist in mosquitoes. Notably, the phenotypes observed upon iron disruption parallel several aspects of human iron-deficiency biology, including altered microbial composition, compromised reproductive capacity, and neurochemical imbalance. These cross-kingdom similarities underscore the evolutionary conservation of iron-dependent pathways and reinforce the broader biological relevance of our findings.

 doi:10.20944/preprints202602.0119.v1

While the study provides a comprehensive functional framework, limitations remain—including the use of transient RNAi knockdowns and the species-specific role of the microbes in iron-regulation. Future genetic, biochemical, and single-mosquito microbiome approaches will be essential to refine the mechanistic pathways uncovered here. Overall, this work positions iron metabolism as a convergence point for multiple physiological systems and identifies it as a promising target for next-generation vector-control strategies.

Acknowledgments: We would like to thank the ICMR-National Institute of Malaria Research insectary staff members for mosquito rearing. We thank Kunwarjeet Singh, Sattey Singh, Lupin, Nishant for their technical assistance in the laboratory.We also thank MOLSYS SCIENTIFIC for WGS shotgun sequencing.

Funding: Laboratory work was supported by the ICMR Grant (Ref # VBD/NIMR/Intra/002-ECD-II). Pooja Yadav is the recipient of UGC fellowship (Ref # 191620022266). The funders had no role in study design, data collection and analysis, decision to publish, or preparation of the manuscript.

Authors contribution: PY, SK, ST and RD conceived and designed the experiments; PY, JR, VS, PR, VS, NS, GS, TS, and GT helped to perform the experiments, drafting and editing MS; PY, JR, SK, ST, RD Contributed reagents/materials/analysis tools, helped in writing, editing, reviewing and finalizing MS.

Competing interest: The authors declare no conflicts of interest.

Data and material availability: The metagenomic sequence data have been submitted to the NCBI SRA database under the following accession numbers: SAMN47311708, DNA_AC_BF_MG, and AC_Fer+Trf_KD_BF_MG described in the manuscript. Transcripts, namely, ferritin, transferrin, hepcidin, and ceruloplasmin, were identified from pre-existing hemocyte RNA-Seq data submitted to the NCBI with accession numbers AC_HC_SF: SRR12031469 (see Rani et al., 2021).

References:

1. B. E. Holbein, C. Lehmann, Dysregulated iron homeostasis as common disease etiology and promising therapeutic target. *Antioxidants* **12**, 671 (2023).
2. V. A. Kokoza, D. Martin, M. J. Mienaltowski, A. Ahmed, C. M. Morton, A. S. Raikhel, Transcriptional regulation of the mosquito vitellogenin gene via a blood meal-triggered cascade. *Gene* **274**, 47–65 (2001).
3. G. M. Attardo, I. A. Hansen, A. S. Raikhel, Nutritional regulation of vitellogenesis in mosquitoes: implications for anautogeny. *Insect Biochem Mol Biol* **35**, 661–675 (2005).
4. I. A. Hansen, G. M. Attardo, S. D. Rodriguez, L. L. Drake, Four-way regulation of mosquito yolk protein precursor genes by juvenile hormone-, ecdysone-, nutrient-, and insulin-like peptide signaling pathways. *Front Physiol* **5**, 103 (2014).
5. J.-L. Wang, T. T. Saha, Y. Zhang, C. Zhang, A. S. Raikhel, Juvenile hormone and its receptor methoprene-tolerant promote ribosomal biogenesis and vitellogenesis in the Aedes aegypti mosquito. *Journal of Biological Chemistry* **292**, 10306–10315 (2017).
6. T. Das De, P. Sharma, S. Tevatiya, C. Chauhan, S. Kumari, P. Yadav, D. Singla, V. Srivastava, J. Rani, Y. Hasija, K. C. Pandey, M. Kajla, R. Dixit, Bidirectional Microbiome-Gut-Brain-Axis Communication Influences Metabolic Switch-Associated Responses in the Mosquito Anopheles culicifacies. *Cells* **11**, 1–24 (2022).
7. S. R. Whiten, H. Eggleston, Z. N. Adelman, Ironing out the details: exploring the role of iron and heme in blood-sucking arthropods. *Front Physiol* **8**, 1134 (2018).
8. H. Nichol, J. H. Law, J. J. Winzerling, Iron metabolism in insects. *Annu Rev Entomol* **47**, 535–559 (2002).
9. Missirlis F, Oliveira PL. Metal ions in the physiology of insects. Curr Opin Insect Sci. 2022 Dec;54:100965. doi: 10.1016/j.cois.2022.100965.
10. D. J. Kosman, Redox cycling in iron uptake, efflux, and trafficking. *Journal of Biological Chemistry* **285**, 26729–26735 (2010).

 doi:10.20944/preprints202602.0119.v1

11. V. Venkataramani, Iron homeostasis and metabolism: two sides of a coin. *Ferroptosis: Mechanism and Diseases*, 25–40 (2021).
12. R. C. Hider, X. Kong, Iron: effect of overload and deficiency. *Interrelations between essential metal ions and human diseases*, 229–294 (2013).
13. Arosio P. New Advances in Iron Metabolism, Ferritin and Hepcidin Research. Int J Mol Sci. 2022 Nov 25;23(23):14700. doi: 10.3390/ijms232314700.
14. M. J. Gorman, Iron homeostasis in insects. *Annu Rev Entomol* **68**, 51–67 (2023).
15. O. A. C. Talyuli, J. H. M. Oliveira, V. Bottino-Rojas, G. O. Silveira, P. H. Alvarenga, A. B. F. Barletta, A. M. Kantor, G. O. Paiva-Silva, C. Barillas-Mury, P. L. Oliveira, The Aedes aegypti peritrophic matrix controls arbovirus vector competence through HPx1, a heme–induced peroxidase. *PLoS Pathog* **19**, e1011149 (2023).
16. G. O. Paiva-Silva, C. Cruz-Oliveira, E. S. Nakayasu, C. M. Maya-Monteiro, B. C. Dunkov, H. Masuda, I. C. Almeida, P. L. Oliveira, A heme-degradation pathway in a blood-sucking insect. *Proceedings of the National Academy of Sciences* **103**, 8030–8035 (2006).
17. A. B. Walter-Nuno, M. L. Taracena, R. D. Mesquita, P. L. Oliveira, G. O. Paiva-Silva, Silencing of iron and heme-related genes revealed a paramount role of iron in the physiology of the hematophagous vector Rhodnius prolixus. *Front Genet* **9**, 19 (2018).
18. D. M. Ward, J. Kaplan, Ferroportin-mediated iron transport: expression and regulation. *Biochimica et Biophysica Acta (BBA)-Molecular Cell Research* **1823**, 1426–1433 (2012).
19. O. Hajdusek, D. Sojka, P. Kopacek, V. Buresova, Z. Franta, I. Sauman, J. Winzerling, L. Grubhoffer, Knockdown of proteins involved in iron metabolism limits tick reproduction and development. *Proceedings of the National Academy of Sciences* **106**, 1033–1038 (2009).
20. G. Zhou, P. Kohlhepp, D. Geiser, M. del C. Frasquillo, L. Vazquez-Moreno, J. J. Winzerling, Fate of blood meal iron in mosquitoes. *J Insect Physiol* **53** (2007).
21. J. Rani, T. Das De, C. Chauhan, S. Kumari, P. Sharma, S. Tevatiya, S. Chakraborti, K. C. Pandey, N. Singh, R. Dixit, Functional disruption of transferrin expression alters reproductive physiology in Anopheles culicifacies. *PLoS One* **17**, 1–17 (2022).
22. V. Bottino-Rojas, L. O. R. Pereira, G. Silva, O. A. C. Talyuli, B. C. Dunkov, P. L. Oliveira, G. O. Paiva-Silva, Non-canonical transcriptional regulation of heme oxygenase in Aedes aegypti. *Sci Rep* **9**, 13726 (2019).
23. M. S. Sonawane, R. C. Salunkhe, R. Z. Sayyed, "Insect gut bacteria and iron metabolism in insects" in *Probiotics, the Natural Microbiota in Living Organisms* (CRC Press, 2021), pp. 343–366.
24. S. Chen, B. K. Johnson, T. Yu, B. N. Nelson, E. D. Walker, Elizabethkingia anophelis: physiologic and transcriptomic responses to iron stress. *Front Microbiol* **11**, 804 (2020).
25. S. He, Y. Qi, The microbiota, the malarial parasite, and the mice—a three-sided relationship. *Front Microbiol* **16**, 1615846 (2025).
26. I. J. Malesza, J. Bartkowiak-Wieczorek, J. Winkler-Galicki, A. Nowicka, D. Dzięciołowska, M. Błaszczyk, P. Gajniak, K. Słowińska, L. Niepolski, J. Walkowiak, The dark side of iron: the relationship between iron, inflammation and gut microbiota in selected diseases associated with iron deficiency anaemia—a narrative review. *Nutrients* **14**, 3478 (2022).
27. H. Bao, Y. Wang, H. Xiong, Y. Xia, Z. Cui, L. Liu, Mechanism of iron ion homeostasis in intestinal immunity and gut microbiota remodeling. *Int J Mol Sci* **25**, 727 (2024).
28. M. S. Medeiros, A. Schumacher-Schuh, A. M. Cardoso, G. V. Bochi, J. Baldissarelli, A. Kegler, D. Santana, C. M. M. B. S. Chaves, M. R. C. Schetinger, R. N. Moresco, Iron and oxidative stress in Parkinson's disease: an observational study of injury biomarkers. *PLoS One* **11**, e0146129 (2016).
29. A. Urati, M. Dey, A. S. Gautam, R. K. Singh, Iron-induced cellular in vitro neurotoxic responses in rat C6 cell line. *Environ Toxicol* **37**, 1968–1978 (2022).
30. H. R. Sanders, A. M. Evans, L. S. Ross, S. S. Gill, Blood meal induces global changes in midgut gene expression in the disease vector, Aedes aegypti. *Insect Biochem Mol Biol* **33**, 1105–1122 (2003).
31. P. Ridwan, The Association between Serum Ferritin and the Gut Microbiome in Patients with Active Tuberculosis Disease in South India. (2019).
32. W. Lei, Z. Liu, H.-P. Lai, R. Fu, Gut microbiota and risk of iron deficiency anemia: A two-sample Mendelian randomization study. *Medicine* **104**, e41617 (2025).

 doi:10.20944/preprints202602.0119.v1

33. A. B. Lange, I. Orchard, F. M. Barrett, Changes in haemolymph serotonin levels associated with feeding in the blood-sucking bug, Rhodnius prolixus. *J Insect Physiol* **35**, 393–399 (1989).
34. J. Zheng, J. Xu, R. Zhang, J. Du, H. Wang, J. Li, D. Zhou, Y. Sun, B. Shen, MicroRNA-989 targets 5-hydroxytryptamine receptor1 to regulate ovarian development and eggs production in Culex pipiens pallens. *Parasit Vectors* **16**, 326 (2023).
35. L. Gao, B. Zhang, Y. Feng, W. Yang, S. Zhang, J. Wang, Host 5-HT affects Plasmodium transmission in mosquitoes via modulating mosquito mitochondrial homeostasis. *PLoS Pathog* **20**, e1012638 (2024).
36. C. S. Benson, A. Shah, M. C. Frise, C. J. Frise, Iron deficiency anaemia in pregnancy: a contemporary review. *Obstet Med* **14**, 67–76 (2021).
37. A. Ferreira, P. Neves, R. Gozzelino, Multilevel impacts of iron in the brain: the cross talk between neurophysiological mechanisms, cognition, and social behavior. *Pharmaceuticals* **12**, 126 (2019).
38. T. Ganz, Hepcidin and iron regulation, 10 years later. *Blood, The Journal of the American Society of Hematology* **117**, 4425–4433 (2011).
39. V. Sangkhae, E. Nemeth, Regulation of the iron homeostatic hormone hepcidin. *Advances in nutrition* **8**, 126–136 (2017).
40. T. Das De, P. Sharma, C. Rawal, S. Kumari, S. Tavetiya, J. Yadav, Y. Hasija, R. Dixit, Sex specific molecular responses of quick-to-court protein in Indian malarial vector Anopheles culicifacies: conflict of mating versus blood feeding behaviour. *Heliyon* **3** (2017).
41. N. Dzaki, K. N. Ramli, A. Azlan, I. H. Ishak, G. Azzam, Evaluation of reference genes at different developmental stages for quantitative real-time PCR in Aedes aegypti. *Sci Rep* **7**, 43618 (2017).
42. T. H. Ahmed, T. R. Saunders, D. Mullins, M. Z. Rahman, J. Zhu, Molecular action of pyriproxyfen: Role of the Methoprene-tolerant protein in the pyriproxyfen-induced sterilization of adult female mosquitoes. *PLoS Negl Trop Dis* **14**, e0008669 (2020).
43. S. Kumari, S. Tevatiya, J. Rani, T. Das De, C. Chauhan, P. Sharma, R. Sah, S. Singh, K. C. Pandey, V. Pande, A testis-expressing heme peroxidase HPX12 regulates male fertility in the mosquito Anopheles stephensi. *Sci Rep* **12**, 2597 (2022).
44. M. Teufel, P. Sobetzko, Reducing costs for DNA and RNA sequencing by sample pooling using a metagenomic approach. *BMC Genomics* **23**, 613 (2022).
45. S. Chen, Y. Zhou, Y. Chen, J. Gu, fastp: an ultra-fast all-in-one FASTQ preprocessor. *Bioinformatics* **34**, i884–i890 (2018).
46. P. T. L. C. Clausen, F. M. Aarestrup, O. Lund, Rapid and precise alignment of raw reads against redundant databases with KMA. *BMC Bioinformatics* **19**, 1–8 (2018).
47. D. Li, C.-M. Liu, R. Luo, K. Sadakane, T.-W. Lam, MEGAHIT: an ultra-fast single-node solution for large and complex metagenomics assembly via succinct de Bruijn graph. *Bioinformatics* **31**, 1674–1676 (2015).
48. P. T. West, A. J. Probst, I. V Grigoriev, B. C. Thomas, J. F. Banfield, Genome-reconstruction for eukaryotes from complex natural microbial communities. *Genome Res* **28**, 569–580 (2018).
49. R. R. Ajjuri, J. M. O'Donnell, Novel whole-tissue quantitative assay of nitric oxide levels in Drosophila neuroinflammatory response. *J Vis Exp*, 50892 (2013).